BOREAL ENVIRONMENT RESEARCH 14 (suppl. A): 86–109
ISSN 1239-6095 (print) ISSN 1797-2469 (online)

Helsinki 27 April 2009

The urban measurement station SMEAR III: Continuous monitoring of air pollution and surface–atmosphere interactions in Helsinki, Finland

Leena Järvi[1)], Hanna Hannuniemi[1)], Tareq Hussein[1)], Heikki Junninen[1)], Pasi P. Aalto[1)], Risto Hillamo[2)], Timo Mäkelä[2)], Petri Keronen[1)], Erkki Siivola[1)], Timo Vesala[1)] and Markku Kulmala[1)]

[1)] *Department of Physics, P.O. Box 64, FI-00014 University of Helsinki, Finland*
[2)] *Finnish Meteorological Institute, Research and Development, P.O. Box 503, FI-00101 Helsinki, Finland*

Received 31 Jan. 2008, accepted 29 May 2008 (Editor in charge of this article: Veli-Matti Kerminen)

Järvi, J., Hannuniemi, H., Hussein, T., Junninen, H., Aalto, P. P., Hillamo, R., Mäkelä, T., Keronen, P., Siivola, E., Vesala, T. & Kulmala, M. 2009: The urban measurement station SMEAR III: Continuous monitoring of air pollution and surface–atmosphere interactions in Helsinki, Finland. *Boreal Env. Res.* 14 (suppl. A): 86–109.

We present results from the air pollution and turbulent exchange measurements made at the urban measurement station SMEAR III in Helsinki, Finland. First measurements at the station started in August 2004 and since then more measurements have gradually been added. We analyze data until June 2007. Temporal variations and dependencies between the size-fractionated particle number concentrations (both fine and coarse particle concentrations), gas concentrations (O_3, NO_x, CO and SO_2), turbulent fluxes of momentum, sensible and latent heat and CO_2, and meteorological variables were studied. Most of the air pollutants and turbulent fluxes showed distinct annual and diurnal variation closely related to the local combustion sources (especially traffic) and the amount of available solar radiation. Ultrafine particles showed the most explicit dependence on traffic and traffic-related pollutants, while larger particles were more affected by the meteorological conditions. The surface fluxes were strongly affected by the specific conditions in urban environment.

Introduction

As compared with natural areas, urban areas create very different circumstances for the lowest level of the atmosphere. Most of the air pollution sources (both aerosol particle and gaseous pollutant sources) are concentrated in urbanized areas where also majority of people live and the adverse health effects of air pollutants get the greatest interest. In addition, cities are characterized by high roughness of the surface and different thermal conditions (Urban heat island effect, Oke 1982), both affecting the spatial and temporal behaviour of wind field and the strength of turbulent exchange including the turbulent fluxes of momentum, energy and matter (Roth 2000, Oke *et al*. 1989). These have further effect on pollutant dispersion (Hanna and Britter 2002).

Previously, atmospheric pollution was linked with many type of health problems including cardiopulmonary and respiratory diseases (e.g. Curtis *et al*. 2006). In addition, air pollutants

affect visibility and climate (Seinfeld and Pandis 1998). For example ultrafine particles (UFP, aerodynamic diameter $d < 0.1$ μm) can affect human health by penetrating deep into lungs and blood circulation (e.g. Nel 2005), and can act as cloud condensation nuclei and affect cloudiness. In urban areas, UFP are mainly produced in combustion processes which include both traffic and stationary emission sources (e.g. Young and Keeler 2007). UFP can be emitted as a primary emission or can be produced in secondary reactions from precursor vapours. Nucleation of aerosol particles may also occur without anthropogenic precursors and the observations of nucleation events cover various environments from clean arctic areas to polluted cities as reviewed by Kulmala *et al*. (2004). Accumulation mode particles ($0.1 < d < 1$ μm) can also be produced in combustion processes but, contrary to UFP, their size is favourable for long-range transport (LRT) in the atmosphere. Coarse particles ($d > 1$ μm) are mainly re-suspended dust from soil and roads by natural and traffic induced turbulence.

Despite the effects of air pollution, information concerning the sources, sinks, mixing and chemistry of air pollutants in urban areas is still lacking. So far, the simultaneous measurements of size-fractioned particle number concentrations and gas pollutant concentrations have been made in Europe (e.g. Ruuskanen *et al*. 2001, Wehner and Wiedensohler 2003, Ketzel *et al*. 2004, Aalto *et al*. 2005, Hussein *et al*. 2006), North America (e.g. Noble *et al*. 2003, Jeong *et al*. 2004, Young and Keeler 2007), Australia (e.g. Morawska *et al*. 1998) and Asia (e.g. Shi *et al*. 2007), but the measured variables and the length of the measurements varied strongly. Also the measurements of turbulent exchange have been restricted to few cities in industrialized countries (Grimmond and Oke 2002, Nemitz *et al*. 2002, Soegaard and Møller-Jensen 2003, Grimmond *et al*. 2004, Moriwaki and Kanda 2004, Vogt *et al*. 2006, Coutts *et al*. 2007, Vesala *et al*. 2007). The direct measurements of turbulent fluxes in urban areas are required, not only for the better knowledge of turbulent processes in urban environments and their effect on pollutant dispersion, but also because urban areas cause friction in the above air and can affect mesoscale weather phenomena and local weather forecasts (e.g. Coceal and Belcher 2004). Previously, ESCOMPTE campaign brought together simultaneous measurements of turbulent fluxes, aerosol particle number and gas concentrations in Marseille, France, but the campaign was limited to summer 2000 (Cros *et al*. 2004).

The urban measurement station SMEAR III (Station for Measuring Ecosystem–Atmosphere Relationships) was established in Helsinki, Finland, in autumn 2004. The station is an extension to the other SMEAR stations located in different surroundings around Finland (Fig. 1a). The purpose of the SMEAR station network is to measure the exchange of momentum, energy and matter in different environments, and to obtain continuous long-term measurements covering chemical and physical properties of atmospheric aerosols, gas pollutants, turbulent exchange and basic meteorology. The SMEAR I station is located in Värriö (67°46´N, 29°36´E), eastern Lapland, close to the Russian border and it represents a remote location where the amount of local emissions is very low (Hari *et al*. 1994). The SMEAR II station is a rural background station located in Scots pine forest near Hyytiälä Forestry field station in southern Finland (61°51´N, 24°17´E) (Hari and Kulmala 2005). The SMEAR III station extended the measurement network into the city of Helsinki where the station is situated at two urban background locations (Fig. 1b). The air pollution measurements together with the meteorological and turbulent exchange measurements are made in Kumpula, 5 km northeast of the Helsinki centre, while the multidisciplinary ecosystem research is made in Viikki, about 7 km northeast of the Helsinki centre. The station is operated together with the University of Helsinki and the Finnish Meteorological Institute (FMI). To our knowledge, this is the first time when simultaneous continuous long-term measurements of turbulent parameters and broad aerosol particle size spectrum (starting from 3 nm particles) are made in the same place in urban areas.

In this study, we focus on the air quality and turbulent exchange measurements made at the Kumpula site. At that site, the number size distribution of fine aerosol particles (UFP + accumulation mode particles; d = 3–950 nm) and basic meteorological variables have been measured since August 2004. Since then, measurements

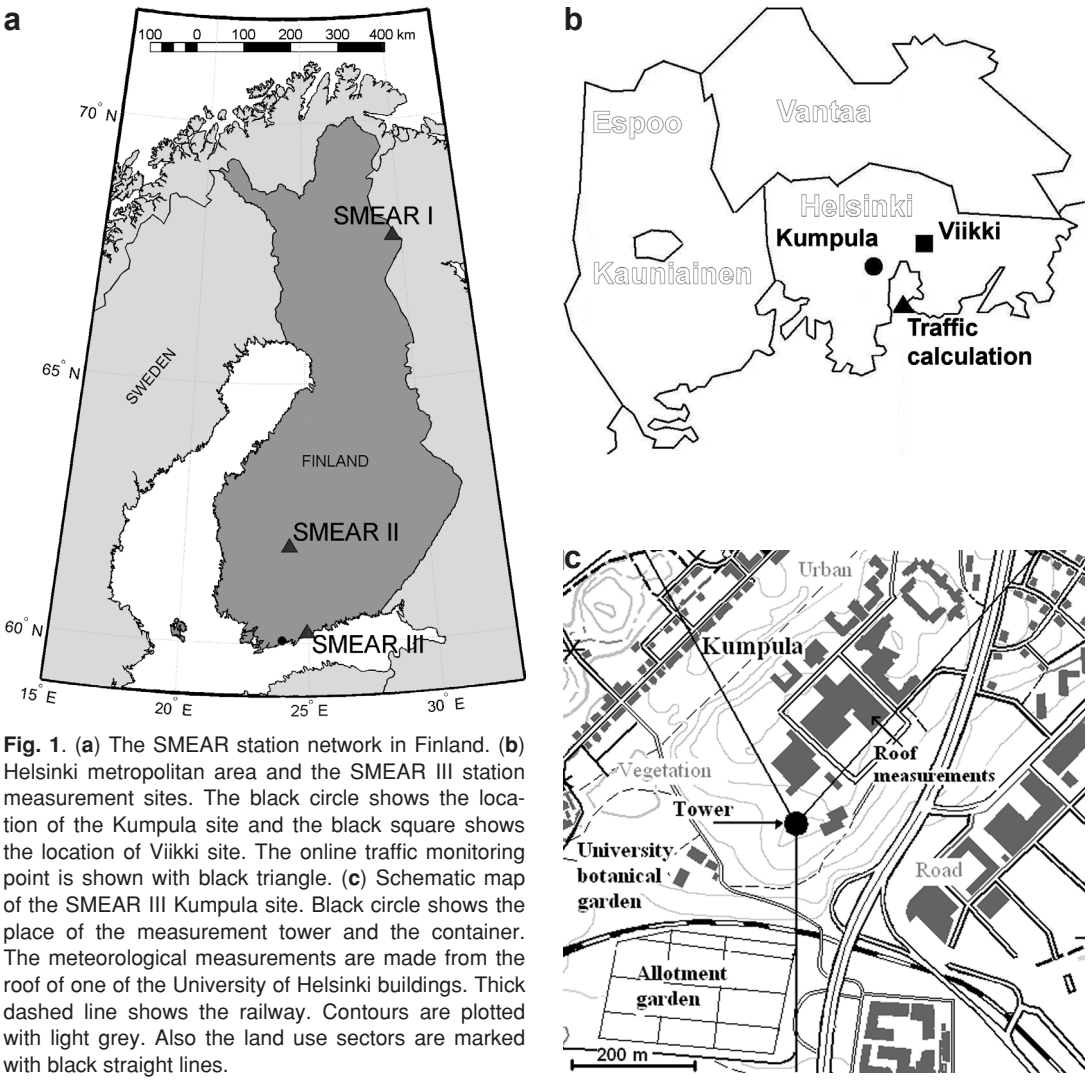

Fig. 1. (**a**) The SMEAR station network in Finland. (**b**) Helsinki metropolitan area and the SMEAR III station measurement sites. The black circle shows the location of the Kumpula site and the black square shows the location of Viikki site. The online traffic monitoring point is shown with black triangle. (**c**) Schematic map of the SMEAR III Kumpula site. Black circle shows the place of the measurement tower and the container. The meteorological measurements are made from the roof of one of the University of Helsinki buildings. Thick dashed line shows the railway. Contours are plotted with light grey. Also the land use sectors are marked with black straight lines.

have been extended to coarse particle (1–20 μm) number concentration, pollutant gas concentrations (O_3, NO_x, CO and SO_2) and turbulent fluxes of momentum, heat, H_2O and CO_2. We utilized measurements of these variables until June 2007, covering all four seasons. During the analyzed periods, we studied temporal behaviour (with annual and diurnal timescales) of aerosol particle number concentrations, gas concentrations, meteorology and turbulent fluxes. We also investigated wind direction dependencies of pollutant concentrations, and a multiple linear regression (MLR) analysis was made to find the variables affecting different size-fractionated aerosol particles. In the analysis, the effect of traffic rates and meteorological variables (including turbulent fluxes) were studied. In addition, correlations between gas concentrations and number concentrations of UFP and accumulation mode particles were analyzed.

Materials and methods

Site description

The SMEAR III station was officially started in Helsinki in autumn 2004. Helsinki is located on

a relatively flat land on the coast of the Gulf of Finland, and together with the three neighbouring cities (Espoo, Vantaa and Kauniainen) Helsinki forms the Helsinki Metropolitan area with an area of 765 km^2 and approximately one million inhabitants. The climate in southern Finland can roughly be classified as either marine or continental depending on the air flows and pressure systems. Either way, the weather is milder than typically at the same latitude (60°N) mainly due to the Atlantic Ocean and the warm Gulf Stream. In Helsinki, the 30-year (1971–2000) monthly-average temperatures range from –4.9 °C in February to 17.2 °C in July (Drebs *et al*. 2002). The yearly precipitation is 642 mm being highest in late summer and lowest in spring.

The air pollution and turbulent exchange measurements are made at an urban background location in Kumpula about 5 km northeast of the Helsinki centre. The turbulent fluxes are measured on the 31-m-high, triangular lattice tower located on a rocky hill (60°12´N, 24°58´E, 26 m above sea level) next to the University of Helsinki buildings and the Finnish Meteorological Institute (Fig. 1c). Next to the tower, an air-conditioned measurement container is located, where the aerosol particle and the trace gas measurement instrumentation is located. In addition, basic meteorological measurements are made from the roof of University of Helsinki buildings (Fig. 1c).

The surroundings of the tower and the container are very heterogeneous consisting of buildings, parking lots, roads, patchy forest and low vegetation. The area around the tower (within a circle of radius 250 m) has 14% coverage of buildings, 40% coverage of asphalted area and 46% coverage of vegetation. The land use is not evenly distributed and the surrounding area can be divided into three land use sectors: urban (320°–40°), road (40°–180°) and vegetation sector (180°–320°). The FMI and the campus area of University of Helsinki are located in the urban sector where the building coverage is 42%. The mean height of the buildings is 20 metres, and the closest of them is situated 55 metres away from the tower. The space between is covered with parking lots with traffic activity mainly on weekdays. In the urban sector the fraction of asphalted area is 51%. A residential area with one-family houses and green spaces is located behind the campus area. The traffic loads on the small roads of the area are low, and the largest source of atmospheric pollutants is the residential activity including wood combustion. The road sector is dominated by one of the main roads leading to the centre of Helsinki. The average daily traffic intensity is 50 000 vehicles and the amount of heavy duty vehicles on that road is considerable. The tower and the road are separated by a belt of deciduous forest with a width of 150 metres. The other side of the road is covered by buildings and sea at a distance of one kilometre (Fig. 1c). In the road sector, 60% of the surface is covered by asphalted area, 30% by vegetation and 10% by buildings. The vegetation sector is mainly covered by green spaces (85%) and fractions of roads and buildings are only 13% and 2%, respectively. Nearby area of the tower is covered by deciduous forest and behind that is an area of grasses, walkways and gardens in an allotment garden and the University Botanical garden. On the other side of the allotment garden (600 metres), the more urbanized area starts with blockhouses and roads. A railway, with a couple of trains per day, leading to Helsinki harbour is passing through the vegetation sector.

Measurements (*see* also Table 1)

Aerosol particle concentrations

The aerosol particle size range from 3 to 950 nm has been measured with a twin differential mobility particle sizer (DMPS, e.g. Aalto *et al*. 2001) since spring 2004. The DMPS technique is based on the bipolar charging of aerosol particles, followed by classification of particles into size classes according to their electrical mobility with a differential mobility analyzer (DMA). The number of particles in each size class is counted with a condensation particle counter (CPC). In our setup, one DMPS measures particles in the size range of 3–50 nm and it consists of a Hauke-type DMA (10.9 cm in length) and a TSI Model 3025 CPC. The sample and sheath flows are 3 and 171 l min^{-1}, respectively. The other DMPS measures particles in the size range of 10–950 nm with a Hauke-type DMA (28 cm in length)

Table 1. Summary of the used parameters and their measurement setups.

Measured quantity	Technique	Equipment	Measurement resolution	Detection limit
Particle concentration with size range 3–950 nm	Twin differential mobility particle sizer	Hauke-type DMA (10.9 cm) + TSi Model 3025 CPC Hauke–type DMA (28 cm) + TSi Model 3010 CPC	10 min	
Particle concentration with size range 0.5–20 µm	Aerodynamic Particle Sizer (APS)	TSI Model 3321	10 min	
Three wind components and temperature	3-D ultrasonic anemometer	Metek USA-1	0.1 s	
Friction velocity, sensible and latent heat fluxes, CO_2-flux	Eddy Covariance (EC)	Metek USA-1 + Open-path infrared absorption gas analyzer (LI–7500)	0.1 s	
Wind direction	2-D ultrasonic anemometer	Thies Clima ver. 2.1x	10 s	
Air temperature	Platinum resistance thermometer	Pt-100	60 s	
Global radiation and photosynhetically active radiation (PAR)	Net radiometer and photodiode sensor	Kipp & Zonen CNR1 + PAR lite	60 s	
Relative humidity	Platinum resistance thermometer + thin film polymer sensor	Vaisala DPA500	4 min	
Air Pressure	Barometer	Vaisala HMP243	4 min	
NO_x	Chemiluminescence technique + thermal (molybdenum) converter	TEI42S	60 s	0.2 ppb
O_3	IR-absorption photometer	TEI 49	60 s	0.5 ppb
CO	Non-dispersive infrared (NDIR) absorption technique	Horiba APMA 370	60 s	20 ppb
SO_2	UV-fluorescence technique	Horiba APSA 360	60 s	0.2 ppb

and a TSI Model 3010 CPC. For this system, the sample and sheath flows are 1 and 5 l min^{-1}, respectively. Each sheath flow is arranged as a closed loop with an air filter and aerosol dryer. The sampling line is 2-m-long stainless steel tube with inner diameter of 4 mm and aerosol flow rate of 4 l min^{-1}. Sampled air is drawn outside the measurement container from the height of four metres. Time resolution of the combined system is 10 minutes (*see* also Aalto *et al*. 2001).

The aerosol particle size range from 0.5 to 20 μm has been measured with an aerodynamic particle sizer (APS, TSI3321) since May 2005. The APS classifies aerosol particles by using a

time-of-flight measurement to measure the aerodynamic diameter. The sample flow was 1 l min^{-1} and sheath flow 4 l min^{-1} for the APS, which had a separate sampling line. The time resolution of the measurements is 10 minutes.

Gas pollutants

Concentrations of nitrogen oxides (NO_x) and ozone (O_3) have been measured with a chemiluminescence analyser (TEI42S, Thermo Environmental Instruments Inc., MA, USA) and an IR-absorption photometer (TEI49, Thermo Environmental Instruments Inc., MA, USA), respectively, since November 2005. The measurements of sulphur dioxide (SO_2) started with a UV fluorescence analyser (APSA 360, Horiba, Kyoto, Japan) in September 2006 and the measurements of carbon monoxide (CO) with an IR-absorption analyser (Horiba APMA 370, Horiba, Kyoto, Japan) in December 2006. In gas measurements, time resolution of one minute is used.

Turbulent fluxes and meteorological variables

The turbulent fluxes of momentum, sensible and latent heat, and CO_2 have been measured with an eddy covariance (EC) technique on top of the tower at the height of 31 metres since December 2005. The EC setup includes a Metek ultrasonic anemometer (USA-1, Metek GmbH, Germany), which measures all three wind components and sonic temperature, and an open path infrared gas analyzer (LI-7500, Li-Cor Inc., Lincoln, Nebraska, USA) to measure carbon dioxide and water vapour mixing ratios. The gas analyzer is connected to the anemometer data logger for synchronization and the raw data is stored for calculation of turbulent fluxes. Measurement frequency of the EC measurements is 10 Hz.

Besides the EC system, the horizontal wind speed components and wind direction have been measured on top of the tower with a 2-dimensional ultrasonic anemometer (Thies CLIMA ver. 2.1x, Goettingen, Germany) since November 2004 with time resolution of 10 seconds. From the same level, air temperature has been measured with a platinum resistant thermometer (Pt-100) since May 2005, and total solar radiation and PAR (photosynthetically active radiation) with a net radiometer and photodiode sensor (CNR1 + PAR lite, Kipp & Zonen, Delft, the Netherlands), respectively, since July 2005. Time resolution for all of these is one minute. Air pressure and relative humidity are measured with a barometer (Vaisala DPA500, Vaisala Oyj, Vantaa, Finland), and platinum resistance thermometer and thin film polymer sensor (Vaisala HMP243, Vaisala Oyj, Vantaa, Finland) from the roof of University of Helsinki Building (Fig. 1c), respectively, with a time resolution of four minutes.

Traffic monitoring

Traffic rates in Helsinki metropolitan area are monitored by the Helsinki City Planning Department. The nearest continuous calculation point is on Itäväylä road, about 2.5 km south from the measurement site (Fig. 1b). The traffic monitoring does not take into consideration the split between light- and heavy-duty vehicles. Traffic data are logged at 1-hour intrvals, except during rush hours when the logging interval is 15 minutes. Hourly values were calculated for December 2005–August 2007.

Data treatment

We divided the aerosol particle size spectrum into three size classes: ultrafine (3–100 nm), accumulation mode (100 nm–1 μm) and coarse particles (1–20 μm). The separation was made due to the deviations in origin, chemical composition and physical properties of different sized particles. The UFP and accumulation mode particle concentrations were obtained from the twin DMPS and the number of coarse particle from the APS. Since the DMPS and APS have different measurement principles, we converted the aerodynamic diameters measured with APS to the diameters equivalent with DMPS measures. This was done by dividing the aerodynamic diameter with a square root of the effective density of the aerosol particles. The effective density

value of 1.5 g cm^{-3} was used in this study (Stein *et al*. 1994, McMurry *et al*. 2002, Khlystov *et al*. 2004). A sensitivity test showed that with effective density value ± 0.25 g cm^{-3}, we get differences from 14% to 27% in coarse particle concentrations depending on the season. For aerosol particle measurements, data from May 2005 to June 2007 was analyzed (if not mentioned otherwise) and for this period the data coverage's were over 96% and 82% for twin DMPS and APS, respectively. Half-hour medians were calculated for pollutant concentrations (both aerosol particle number and gas concentrations). The only exception was the multiple linear regression analysis when hourly values were used due to the measurement resolution of traffic rates.

Turbulent fluxes were calculated as averages of the covariance of vertical wind speed and considered scalar, according to common procedures presented by Aubinet *et al*. (2000). Before the flux calculations, data was de-trended and a 2-dimensional coordinate rotation was applied. Fluxes were also corrected for water vapour and heating effects according to Webb *et al*. (1980). Clear peaks were removed by visual inspection and a stationary test was performed (Foken and Wichura 1996), where the 30-minute interval used for the calculation of one flux point is compared with the same interval divided into six subintervals. If the difference between these two was more than 60%, the flux data point was rejected as non-stationary. The flux data was filtered against friction velocity (u_*) and data with $u_* <$ 0.1 m s^{-1} was screen out. Flux data from December 2005 to June 2007 were analyzed. Missing data points covered 12% of this period and the amount of rejected data points varied between the fluxes and seasons. For momentum and heat fluxes the amount of rejected data was low, between 3%–15% of the measured data. For CO_2 flux, 20%–50% of the data was rejected while for water vapour the amount was 20%–40%. The amount of rejected data was high, but still typical for EC measurements (e.g. Suni *et al*. 2003). The EC measurements are done in the vicinity of buildings, whose heights are on average 2/3 of the measurement height. This may cause problems for the EC measurements when wind is blowing from the direction of these buildings. However, Vesala *et al*. (2007) showed the basic micrometeorological theories (Monin-Obukhov similarity and spectral theories) applying rather well also downwind from the buildings.

Atmospheric stability ζ is an important derivative obtained from the flux measurements. It describes the dispersion conditions and it is obtained from the relationship between sensible heat and momentum fluxes, which roughly describe the thermal and mechanical turbulence productions, respectively. ζ gets negative values in unstable atmosphere, positive in stable stratified atmosphere and in neutral situations ζ is between –0.01 and 0.01.

Size-fractioned aerosol particle number data and meteorological variables (wind speed, wind direction, pressure, RH, radiation, PAR) were divided according to seasons between May 2005 and Jun 2007, and a definition of thermal seasons was used. Spring and autumn are the periods when daily average temperatures are between 0 and 10 °C, and winter and summer are when the temperatures are below 0 and above 10 °C, respectively. According to this definition winter was found to be from 16 December 2005 to 7 April 2006 and from 19 January to 6 March 2007 with a total number of 160 days. Summer covered 21 May–13 October 2005, 4 June–10 October 2006 and 17 May–30 June 2007 with a total number of 274 days. The number of days in spring and autumn were 148 and 164, respectively. For other variables, same seasonal division was used but for shorter periods. NO_x and O_3 concentrations were analyzed between November 2005 and June 2007, while for SO_2 and CO the analyzed periods covered September 2006–June 2007 and December 2006–June 2007, respectively. The turbulent fluxes were analyzed between December 2005 and June 2007.

Multiple linear regression analysis

Air pollution concentrations are complex functions of sources, sinks, synoptic and mesoscale meteorology, and turbulence, which all vary strongly by time. We tried to distinguish the effect of different variables on measured aerosol particle concentrations by means of a multiple linear regression analysis (MLR). In MLR, a linear relationship between a dependent variable

(in this case the aerosol particle concentration) and several independent variables is studied. The basic idea is to develop a model

$$Y = b_0 + b_1X_1 + \ldots + b_nX_n, \quad (1)$$

where Y is the modelled concentration, $X_1 \ldots X_n$ are independent variables, b_0 is the intercept and $b_1 \ldots b_n$ are regression coefficients (Hair *et al.* 2006). The MLR models were obtained by considering all possible combinations of independent variables, and finding such variables that the difference between the measured and modelled concentrations is minimized. This provides variables $X_1 \ldots X_n$, which are significant concerning the aerosol particle concentrations, and the direction of the dependence. Traffic rate, turbulent fluxes of momentum and heat, wind speed, wind direction, pressure, RH, solar radiation and PAR were taken into account in the analysis.

Normalization of the dependent and independent variables before the model development enables to get so-called beta coefficients, which tell the relative importance of each independent variable to the dependent variable as compared with other independent variables in the model. We used bootstrapping to obtain uncertainties for model parameters and performance indices and to have results more representative. In bootstrapping, original data set is divided into 100 subsets each including arbitrary 5/6 of the data set. Separate MLR models are developed to each subset and the beta coefficients, R^2 and root mean square error are calculated as arithmetic means from these submodel parameters.

In order to use MLR, used variables should be normally distributed. However, some of the variables were not distributed normally and therefore data transformations to correct the non-normality were used. Logarithmic transformations were used for aerosol particle number and H_2O concentrations. For wind direction components, radiation variables (total solar radiation and PAR) and stability parameter, inverse transformations were applied. Finally, traffic rates were square-transformed. MLR analysis was made separately for UFP, accumulation mode particle and coarse particle number concentrations. Due to limited amount of traffic and turbulent flux data, only data between December 2005 and August 2006 were used. Analysis was done for hourly median values (for fluxes average values were used) and only dry hours were taken into account. The analyzed data accounted 60% of the period.

Results and discussion

Annual variations of aerosol particle number and gas pollutant concentrations

The highest UFP and NO_x concentrations were systematically measured in late winter (February–March) when the concentrations were around 13 000 cm^{-3} and 18 ppb (Fig. 2). For CO and SO_2, data over only one year existed and during that time they had maxima (270 and 1.5 ppb, respectively) also in late winter. The elevated concentrations are caused by the lowered mixing in the boundary layer and also enhanced emissions from combustion sources (mainly stationary emission sources) during the coldest periods which usually occur in February (Drebs *et al.* 2002). NO_x, CO and SO_2 are all emitted in fossil fuel burning processes and in the case of NO_x and CO this mainly refers to traffic while in the case of SO_2 the main source is energy production. More efficient boundary layer mixing could be seen as lowered UFP, NO_x and CO concentrations in summer. Previously also Woo *et al.* (2001) and Aalto *et al.* (2005) showed higher UFP concentrations in winter than in summer.

Concentrations of UFP and NO_x were systematically higher on weekdays than on weekends (Table 2). In the case of CO, the same pattern could be seen in winter. The difference between the weekday and weekend concentrations is caused by additional traffic on weekdays. This was pronounced in winter when the poor mixing conditions cause traffic emissions to be more evidently detected at the measurement point. In spring and summer, deviations between weekday and weekend concentrations were smaller. In the case of UFP, the difference can be smoothed by the nucleation of new particles which is most frequent in spring (March–May) and late summer (September) (e.g. Dal Maso *et al.* 2005). A weekday-related source was also evident in

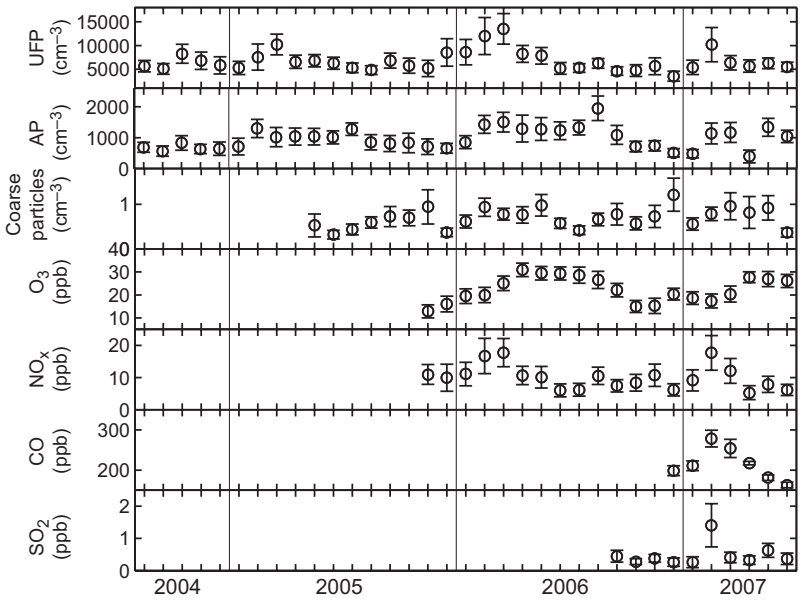

Fig. 2. Monthly medians of number concentrations of ultrafine particles (UFP), accumulation mode particles (AP) and coarse particles, and gas concentrations of ozone (O_3), nitrogen oxides (NO_x), carbon monoxide (CO) and sulphur dioxide (SO_2) in Helsinki in August 2004–June 2007. Error bars show the quartile deviations.

SO_2 concentrations in winter and spring as evidenced by higher weekday concentrations (*see* Table 2). In Finland, the sulphur content of fuels used by road traffic is low (10 ppm since 1995), suggesting that the higher SO_2 concentrations are caused by other weekday-related source, such as power plant activities and residential heating with sulphur-containing fuels. Some effect of traffic cannot, however, be ruled out. Due to the short measurement period of SO_2, these results should be considered with caution.

O_3 experienced its maximum concentration of 30 ppb in spring and early summer, and a minimum concentration of 13 ppb in winter. This annual behaviour of O_3 is strongly related to the amount of available solar radiation and the intensity of photo-oxidation of the precursor gases (Seinfeld and Pandis 1998, Sillman 1999). Contrary to other gases, O_3 concentrations were higher on weekends than on weekdays. Previous studies have reported higher O_3 concentrations outside cities, since inside urban areas O_3 is rapidly consumed in chemical reactions (Sillman 1999, Noble *et al*. 2003). The same phenomenon is likely to explain the lower weekday concentrations.

The annual pattern of accumulation mode particles showed highest concentrations between February and August (Fig. 2). Pronounced peaks were observed in February and in July–August. The winter maximum is related to the lowered mixing and enhanced emissions similarly to UFP. In summer, the accumulation mode particle concentrations are raised by long-range transport (LRT) (Laakso *et al*. 2003) when forest fires/controlled burning typically take place in Russia and eastern Europe bringing polluted air masses to southern Finland (e.g. Sillanpää *et al*. 2005, Rantamäki *et al*. 2007). This was especially pronounced in August 2006 when a maximum concentration of 1800 cm^{-3} was measured. The whole summer 2006 was exceptionally dry and warm, and in August the easterly winds brought highly polluted air masses from extensive wild fires in Russia and Estonia (Rantamäki *et al*. 2007). The accumulation mode particle concentrations were also higher on weekdays than on weekends in winter and spring when the effect of local emissions is more evident due to the lowered mixing. The coarse particles did not have a distinct annual pattern (Fig. 2). However, slightly elevated concentrations (1 cm^{-3}) were measured in spring. This is due to the effective re-suspension of gravelling caused by traffic induced turbulence and wiping machines after melting of snow and ice. Especially, the effect of studded tires on coarse particle concentrations in spring is a well known phenomenon in Scandinavia (e.g. Kupiainen *et al*. 2003, Norman and Johansson 2006, Hussein *et al*. 2008). Coarse parti-

Table 2. The median seasonal statistics for the measured air pollutants: UFP, accumulation mode particle and coarse particle concentrations for May 2005–June 2007, nitrogen oxides (NO_x) and ozone (O_3) for November 2005–June 2007, carbon monoxide (CO) for December 2006–June 2007 and sulphuric dioxide (SO_2) for September 2006–June 2007. Medians were calculated separately for weekdays (Wd) and weekends (We), and division into land use sectors, urban (Urb), road and vegetation (Veg), was made. Quartile deviations (half of the difference between 25 and 75 percentiles) are shown in parentheses.

	Winter				Spring				Summer				Autumn			
	Urb	Road	Veg	All	Urb	Road	Veg	All	Urb	Road	Veg	All	Urb	Road	Veg	All
UFP (10^4 cm^{-3})																
Wd	1.54	1.56	0.77	1.27	0.82	1.06	0.61	0.74	0.68	0.71	0.52	0.59	0.79	0.73	0.47	0.58
	(0.78)	(0.79)	(0.48)	(0.74)	(0.35)	(0.41)	(0.22)	(0.32)	(0.26)	(0.29)	(0.19)	(0.24)	(0.50)	(0.48)	(0.25)	(0.35)
We	0.82	0.90	0.55	0.71	0.53	0.74	0.50	0.58	0.59	0.59	0.44	0.51	0.46	0.47	0.32	0.37
	(0.48)	(0.40)	(0.29)	(0.40)	(0.31)	(0.22)	(0.22)	(0.25)	(0.19)	(0.21)	(0.15)	(0.20)	(0.29)	(0.26)	(0.12)	(0.18)
Accum. particles (10^3 cm^{-3})																
Wd	1.30	1.44	0.88	1.21	0.98	1.72	0.84	1.11	1.14	1.47	1.11	1.22	0.58	0.74	0.53	0.60
	(0.58)	(0.54)	(0.45)	(0.54)	(0.55)	(1.07)	(0.45)	(0.65)	(0.46)	(0.70)	(0.47)	(0.55)	(0.43)	(0.37)	(0.26)	(0.32)
We	0.92	1.29	0.60	0.87	0.45	1.51	0.58	0.75	1.43	1.46	1.07	1.22	0.64	0.87	0.60	0.63
	(0.48)	(0.57)	(0.35)	(0.48)	(0.50)	(0.77)	(0.30)	(0.55)	(0.59)	(0.51)	(0.53)	(0.54)	(0.45)	(0.50)	(0.28)	(0.35)
Coarse particles (cm^{-3})																
Wd	0.78	0.71	0.60	0.71	0.87	0.97	1.09	1.00	0.56	0.72	0.58	0.61	0.49	0.62	0.76	0.65
	(0.32)	(0.29)	(0.30)	(0.30)	(0.57)	(0.41)	(0.68)	(0.53)	(0.29)	(0.34)	(0.34)	(0.35)	(0.29)	(0.52)	(0.62)	(0.51)
We	0.57	0.63	0.49	0.56	0.59	0.82	0.71	0.69	0.34	0.51	0.47	0.46	0.41	0.72	0.87	0.69
	(0.29)	(0.35)	(0.32)	(0.31)	(0.63)	(0.39)	(0.45)	(0.43)	(0.15)	(0.22)	(0.25)	(0.24)	(0.28)	(0.34)	(0.68)	(0.60)
NO_x (ppb)																
Wd	22.2	23.6	15.4	21.8	9.6	19.7	8.0	9.3	6.9	10.5	6.6	8.2	11.1	12.5	7.7	8.9
	(11.0)	(9.8)	(10.1)	(11.1)	(7.8)	(11.6)	(5.5)	(7.4)	(5.0)	(5.9)	(3.5)	(4.5)	(8.3)	(8.5)	(4.2)	(5.5)
We	7.0	8.2	6.6	7.0	2.1	10.4	4.6	5.0	5.7	5.4	5.1	5.2	14.3	9.1	5.5	6.9
	(5.5)	(3.3)	(2.9)	(3.6)	(1.4)	(5.7)	(2.7)	(3.7)	(1.9)	(2.0)	(2.0)	(1.9)	(8.1)	(4.3)	(2.2)	(3.3)
O_3 (ppb)																
Wd	12.4	15.0	15.6	14.5	22.7	20.2	26.9	24.7	22.8	24.9	25.9	25.1	19.1	13.7	20.2	18.2
	(5.1)	(4.9)	(5.5)	(5.6)	(7.1)	(7.4)	(5.5)	(6.5)	(5.8)	(5.9)	(6.5)	(6.6)	(8.0)	(5.8)	(4.5)	(5.7)
We	18.7	28.5	25.6	23.1	27.5	21.0	28.0	27.0	25.4	28.7	32.0	30.5	15.1	14.6	19.2	17.9)
	(5.3)	(2)	(4.2)	(5.0)	(4.4)	(5.4)	(3.3)	(4.5)	(4.8)	(4.8)	(6.0)	(5.5)	(6.8)	(5.8)	(5.0)	(5.9)
CO (ppb)																
Wd	304	302	247	285	226	245	217	217	163	172	163	172	198	211	198	198)
	(46)	(32)	(55)	(44)	(32)	(27)	(23)	(27)	(14)	(18)	(14)	(18)	(19)	(19)	(16)	(13)
We	247	236	217 (30)	236	217	217	199	217	163	163	172	172	229	199	198	198
	(54)	(14)	(30)	(31)	(9)	(27)	(9)	(9)	(11)	(9)	(9)	(9)	(74)	(27)	(19)	(29)
SO_2 (ppb)																
Wd	2.2	0.8	0.6	1.2	0.4	0.7	0.5	0.5	0.3	0.5	0.4	0.4	0.3	0.5	0.3	0.3
	(1.7)	(0.6)	(0.7)	(1.2)	(0.2)	(0.6)	(0.3)	(0.3)	(0.2)	(0.5)	(0.3)	(0.3)	(0.4)	(0.3)	(0.3)	(0.2)
We	0.2	0.6	0.3	0.3	0.2	0.7	0.3	0.29	0.4	0.6	0.5	0.5	0.3	0.5	0.3	0.3
	(0.2)	(0.5)	(0.4)	(0.4)	(0.1)	(0.7)	(0.2)	(0.27)	(0.2)	(0.7)	(0.4)	(0.5)	(0.3)	(0.3)	(0.2)	(0.3)

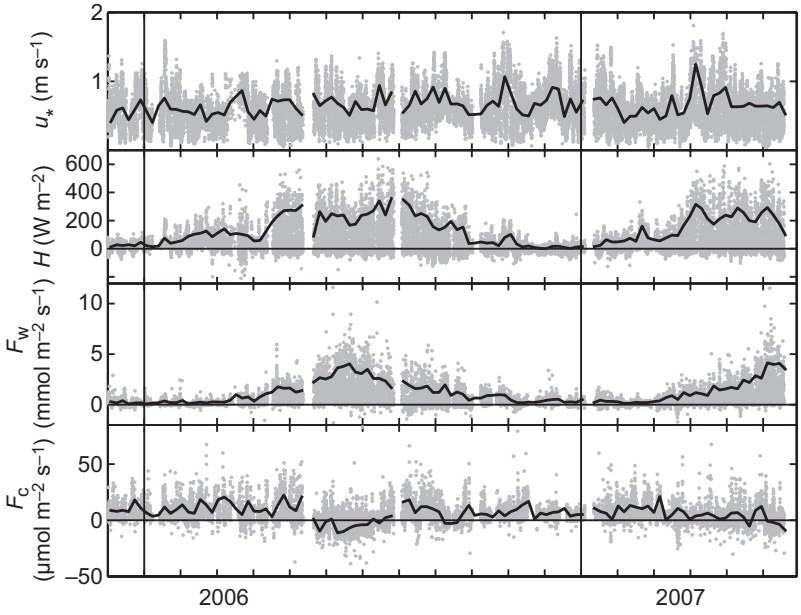

Fig. 3. Time series of the turbulent fluxes (friction velocity u_*, sensible heat flux H, water vapour flux F_w, latent heat flux LE and CO_2 flux F_c) measured in Helsinki in December 2005–June 2007. Grey data points are half-hour averages, and black lines are the daytime (10:00–14:00) median fluxes calculated from five days of data.

cles had also higher concentrations on weekdays (except in autumn) (Table 2), suggesting the effect of traffic induced turbulence and/or some other weekday-related source.

The measured UFP and accumulation mode particle concentrations are comparable to those previously measured in Helsinki and are at the lowest end when compared with those from other cities around the world (Table 3). Coarse particle number concentration measurements were restricted to only few cities and compared with only those, the coarse particle concentrations in Helsinki are low. Also NO_x, CO and SO_2 concentrations were much lower in this study than reported in other urban studies (e.g. Table 3). Klumpp *et al*. (2006) reported O_3 concentrations from 11 European cities and found the concentrations range from 15.5 to 35.3 ppb. Thus, the O_3 concentrations in Helsinki seem to be typical for European cities and are mostly higher than those listed in Table 3. Only few studies reported simultaneous measurements of number concentrations of size-fractioned aerosol particles and gas concentrations (Table 3).

Annual variations of turbulent fluxes

Sensible heat (H) and water vapour (F_w) flux had a clear annual pattern with higher values in summer than in winter (Fig. 3). The median value of H ranged from 20 W m^{-2} in winter to 350 W m^{-2} in summer, while the median value of F_w ranged from near zero in winter to 4 mmol m^{-2} s^{-1} in summer, corresponding to latent heat flux (LE) of 230 W m^{-2}. The measured heat flux values are similar to H and LE measured in a residential area of Tokyo in July, where they reached values of 300 and 200 W m^{-2} (Moriwaki and Kanda 2004), respectively. Grimmond and Oke (2002) presented heat flux data from 10 urban sites in North America and found daily peaks of H ranging from 100 to 300 W m^{-2} and LE ranging from 10 to 240 W m^{-2}. In Basel in summer, H reached a maximum value of 400 W m^{-2} and LE was below 100 W m^{-2} (Vogt *et al*. 2006).

The u_* and CO_2 flux (F_c) did not exhibit a clear annual pattern. Median u_* ranged between 0.4 and 1.5 m s^{-1} and median F_c between –10 and 25 µmol m^{-2} s^{-1}. The anthropogenic emissions (especially from traffic) dominated the CO_2 exchange, masking the background cycle of F_c. The influence of vegetation CO_2 uptake on F_c could only be seen in summer as a downward (negative) fluxes. Our F_c values are comparable to those reported in other studies. In Edinburgh, F_c ranged between 10 and 40 µmol m^{-2} s^{-1} in autumn (Nemitz *et al*. 2002), while in the city of Basel the range was 0–25

Table 3. Median number concentrations of ultrafine particles (UFP), accumulation mode particles (AP) and coarse particles, and median concentrations of ozone (O_3), nitrogen oxides (NO_x), carbon monoxide (CO) and sulphur dioxide (SO_2) from this and other urban studies.

Study	UFP (cm^{-3})	AP (cm^{-3})	Coarse (cm^{-3})	O_3 (ppb)	NO_x (ppb)	CO (ppb)	SO_2 (ppb)	Site description	Comment
This study	10600	1100	0.67	20	14.9	272	0.8	Urban background	Winter
	5600	1200	0.56	26	7.5	172	0.4		Summer
Helsinki, Finland Ruuskanen *et al.* (2001)	15600	905	–	–	–	–	–	Urban background	Winter (UFP: 10–100 nm, AP: 100–500 nm)
Helsinki, Finland Aalto *et al.* (2005)	9500	–	–	–	–	–	–	Urban background	May 2001–Dec 2003 (7–1000 nm)
Alkmaar, Netherlands Ruuskanen *et al.* (2001)	14900	1670	–	–	–	–	–	Urban background	Nov 1996–Mar 1997 (UFP: 10–100 nm, AP: 100–500 nm)
Ashdod, Israel Amoroso *et al.* (2008)	–	–	–	29	17.8	–	1.2	Industrial	Summer 2005
Detroit, Michigan Young and Keeler (2007)	19900	–	–	20	–	830	3.9	Urban	Summer 2003 and 2005 (10–100 nm)
Averages									
Copenhagen, Denmark Ketzel *et al.* 2004	7700	–	–	–	14.8	–	–	Urban background	Sep–Nov 2002 (10–700 nm)
Leipzig, Germany Wehner and Wiedensohler (2003)	19300	2107	–	–	–	–	–	Street canyon	winter weekdays 1997–2001
	13400	1383	–	–	–	–	–		summer weekdays 1997–2001 (UFP: 10–100 nm, AP: 100–800 nm)
El Paso, Texas Noble *et al.* (2003)	14600	2050	3.0	16	78	1100	–	Urban background	winter 1999 (UFP: 20–100 nm, AP: 100–700 nm, Coarse: 1–10 µm)
Atlanta, Georgia Woo *et al.* (2001)	21400	1690	–	25	52	592	5.9	Urban background	1998–1999 (UFP: 3–100 nm, AP: 0.1–2 µm
Brisbane, Australia Morawska *et al.* (1998)	7400	–	4.3	13	34.5	630	4.4	Downtown	Jul 1995–Apr 1997 (UFP: 16–630 nm, Coarse: 0.7–30 µm)

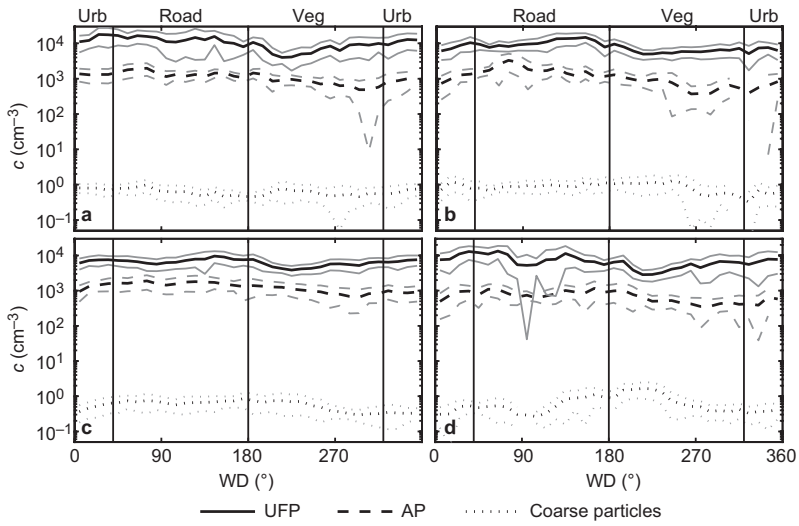

Fig. 4. Dependence of aerosol particle number concentrations on wind direction in (**a**) winter, (**b**) spring (**c**) summer, and (**d**) autumn. Medians for 10° sectors were calculated and plotted on a logarithmic scale. Black solid lines: ultrafine particle (UFP) concentrations, black dashed lines: accumulation mode particle (AP) concentration, black dotted lines: coarse particles. Quartile deviations are indicated with respective grey lines. The land use sectors, urban (Urb), Road and vegetation (Veg) are separated with vertical lines.

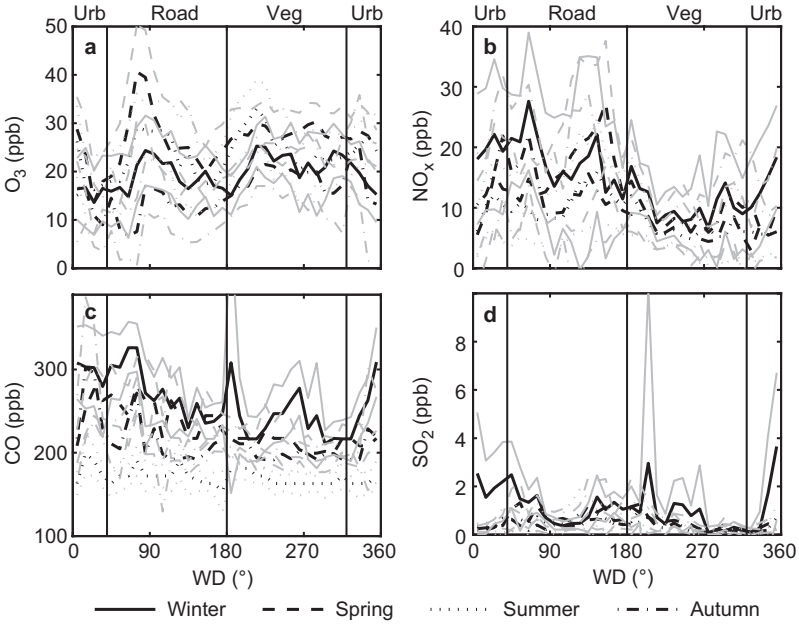

Fig. 5. Seasonal dependence on wind direction of (**a**) ozone (O_3), (**b**) nitrogen oxides (NO_x), (**c**) carbon monoxide (CO), and (**d**) sulphur dioxide (SO_2). Values were calculated as medians from half-hour values for O_3 and NO_x in November 2005–June 2007, for CO in December 2005–June 2007 and for SO_2 in September 2005–June 2007. Grey lines show the respective quartile deviations and the black vertical lines show the land use sectors urban (Urb), road and vegetation (Veg).

μmol m^{-2} s^{-1} in summer. In Chicago and Tokyo in summer, the daily-average fluxes remained below 10 μmol m^{-2} s^{-1}, as reported by Grimmond *et al*. (2002) and Moriwaki and Kanda (2004), respectively. Most of the F_c (and also other turbulent flux) measurements are carried out in urban areas where all four seasons are not as distinguishable as in Finland. Thus in this study, comparisons for winter are quite weak.

Wind direction dependence of aerosol particle number and gas concentrations

The effect of road leading to the centre of Helsinki was evident in the UFP, accumulation mode particle, NO_x and CO concentrations which were higher in the road sector as compared with those in the other land use sectors (Table 2 and Figs. 4–5). In the case of accumulation mode particles and CO, the concentrations in this direction are

also affected by potentially more polluted air masses coming from eastern Europe and Russia. The lowest concentrations of these traffic-related pollutants (UFP, accumulation mode particles, NO_x and CO) were measured in the vegetation sector, where the longest fetch without anthropogenic emission sources is enabled. Pronounced peaks in traffic related pollutants were observed in directions 45°–95° and 100°–170° throughout the year (Figs. 4–5), corresponding directions where largest crossroads are located, and where the coming airflow remains longer above roads (*see* also Fig. 1c). Peak concentrations were also observed downwind from the city centre (180°–190°) which is roughly the direction of the harbour located 6 km away from the measurement site. Ship emissions can affect especially the black carbon part of accumulation mode particles (Pakkanen *et al*. 2001). The UFP, CO and NO_x peaked also in direction 20°–40°. The parking lot, where numerous cars start their engines during the day, is located in this direction. In winter, high concentrations of fine particles, NO_x, CO and SO_2 were measured in the urban sector. This might be related to enhanced domestic activities (wood combustion and oil heating) in the residential area behind the University campus, but also a construction site located less than 100 m north from the measurements may have its own effect on measured pollutant concentrations.

Outside winter time, SO_2 concentrations were slightly higher in the road sector than in the other land use sectors suggesting some effect of traffic (Table 2). Increased SO_2 concentrations were measured downwind from the city centre in direction 130°–250° (Fig. 5). The harbour is also located in this directions and it is likely having its own effect on SO_2 concentrations, since besides energy production sea traffic is an important source of SO_2 in Helsinki (Myllynen *et al*. 2007). Pronounced SO_2 peaks were observed in the directions (140° and 225°) of the two power plants, Hanasaari and Salmisaari.

O_3 and coarse particles did not show distinct dependence on land use sectors (Table 2). Minima in O_3 concentrations were observed in directions 45°–95° and 100°–170° corresponding directions of the crossroads. Likely, the amount of pollutants destroying O_3 is higher in these directions causing the lower O_3 concentrations. The highest coarse particle concentrations were measured downwind from the Botanical Garden (180°–270°) (Fig. 4). The pronounced peak in autumn is likely related to some activity in the garden which causes effective re-suspension of cultivated ground. Small peaks in the direction of the crossroads were also observed in coarse particle concentrations in winter and autumn likely due to re-suspension by traffic induced turbulence.

Diurnal variability of air pollutants, meteorological variables and turbulent fluxes

On weekdays, traffic related pollutants (UFP, accumulation mode particles, CO and NO_x) increased during the morning rush hour (05:00–11:00) and decreased toward the evening (Figs. 6 and 7). Peaks related to afternoon rush hour were evident only occasionally due to the strengthened turbulent mixing in the boundary layer (*see* also Fig. 8h). Similar weekday patterns of UFP with morning maximum have also been observed in Copenhagen (Ketzel *et al*. 2004), Leipzig (Wehner and Wiedensohler 2003) and Belfast (Harrison and Jones 2005). Noble *et al*. (2003) on the other hand found two clear peaks related to morning and afternoon rush hours in UFP, accumulation mode particle, CO and NO concentrations in El Paso, Texas. The effect of lowered mixing could be seen as higher UFP, CO and NO_x concentrations in winter with daily peak values of 24 000 cm^{-3}, 350 ppb and 40 ppb, respectively. In the case of accumulation mode particles, deviations in the diurnal patterns between the seasons were not as much pronounced likely due to the effect of LRT which raised the concentrations especially in summer. This was seen as raised nocturnal (roughly the background) concentrations both on weekdays and weekends. On weekends, UFP, CO and NO_x increased between 10:00–20:00 following the behaviour of traffic activity.

O_3 was clearly sunlight-related with highest concentrations after midday. Similar diurnal behaviour of O_3 has been observed in several European cities (Klumpp *et al*. 2006). The weekday and weekend diurnal patterns deviated

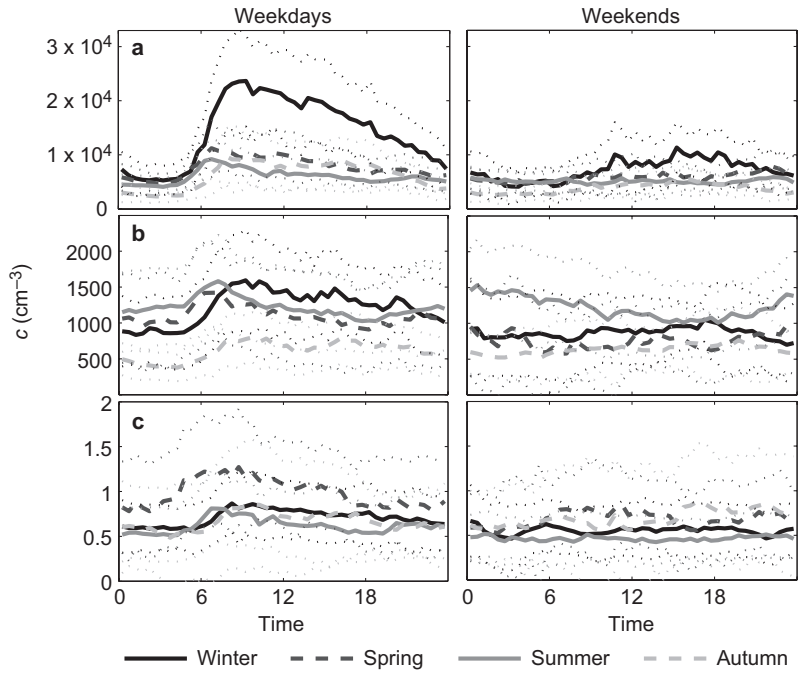

Fig. 6. Median diurnal variation of (**a**) UFP, (**b**) accumulation mode particles (AP), and (**c**) coarse particles separately for weekdays and weekends in May 2005–June 2007. Black line shows the variation in winter, black dashed line in spring, grey line in summer, and grey dashed line in autumn. The quartile deviations for each season are plotted with dotted lines.

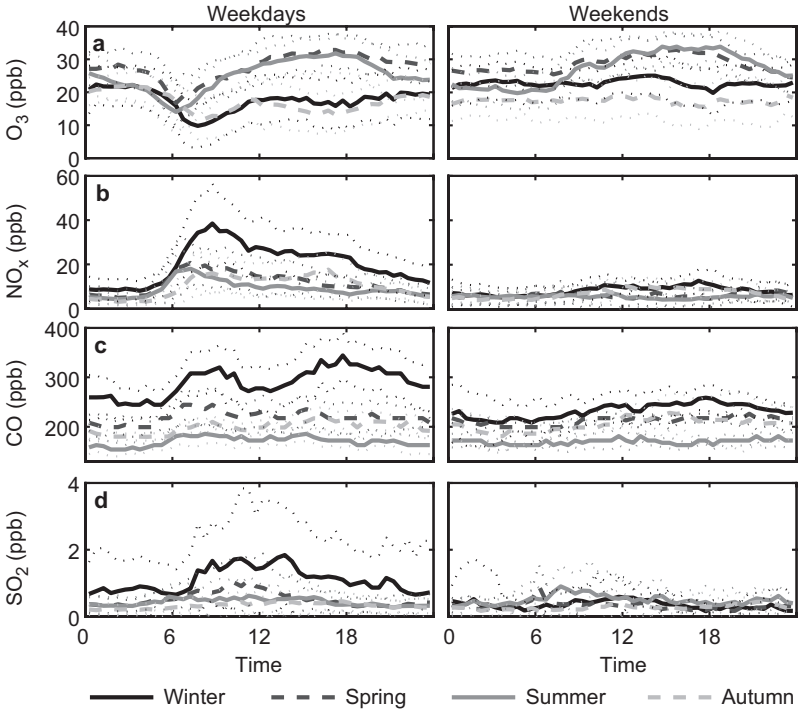

Fig. 7. Median diurnal variation of (**a**) ozone (O_3), (**b**) nitrogen oxides (NO_x), (**c**) carbon monoxide (CO), and (**d**) sulphur dioxide (SO_2) separately for weekdays and weekends. Values were calculated as medians from half-hour values for O_3 and NO_x between November 2005 and June 2007, for CO between December 2005 and June 2007 and for SO_2 between September 2005 and June 2007. Black line shows the variation in winter, black dashed line in spring, grey line in summer, and grey dashed line in autumn. The quartile deviations for each season are plotted with dotted lines.

between 05:00–8:00 when O_3 is rapidly consumed in reactions with other gaseous pollutants on weekdays. Noble *et al*. (2003) found the weekday and weekend diurnal patterns to be nearly equal and the peak O_3 concentration was also observed after midday. The diurnal pattern of SO_2 showed increased daytime concentrations on weekdays which were most pronounced

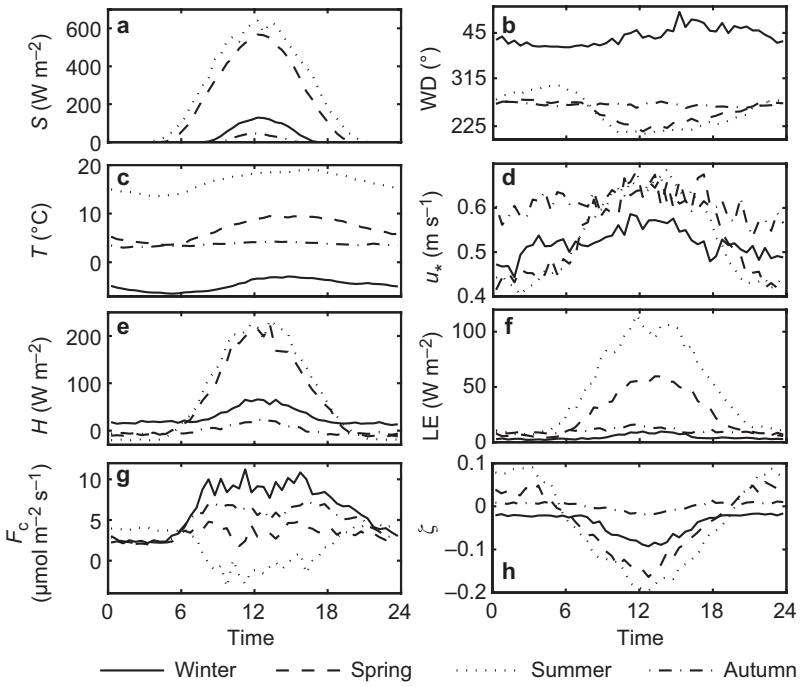

Fig. 8. Median diurnal variation of (**a**) global radiation (S), (**b**) wind direction (WD), (**c**) temperature (T), (**d**) friction velocity (u_*), (**e**) sensible heat flux (H), (**f**) latent heat flux (LE), (**g**) CO_2 flux (F_c), and (**h**) atmospheric stability (ζ) in December 2005–June 2007. Winter values are plotted with solid line, spring values with dashed line, summer values with dotted line and autumn values with dashed-dotted line.

in winter. As previously mentioned, the higher weekday concentrations are related to increased combustion of sulphur-containing fuels and/or the effect of traffic. On weekends, SO_2 did not exhibit any clear diurnal behaviour. A weak effect of traffic could be seen in the diurnal variation of coarse particles during the morning rush hour. The increased coarse particle concentrations caused by traffic and wiping machine induced turbulence could be seen twice as large concentrations in spring than during other seasons. No traffic related pattern could be seen in coarse particle concentration in El Paso, where the peak concentration was measured in the evening (Noble *et al*. 2003).

In Finland, meteorological conditions vary considerably with season and are strongly dependent on the amount of solar radiation (Fig. 8). Note that because of the definition of thermal seasons, the lowest sun radiation values were measured in autumn (Fig. 8a). In Helsinki, also the vicinity of sea has a great effect on the seasonal changes and behaviour of the meteorological variables. In Helsinki, the wind typically blows from west or south-west, except in winter when air flows from Russia (northeastern) are dominating (Fig. 8b). In spring and summer however, the wind direction had a diurnal cycle related to land sea breeze, which is produced by the different heat capacities of sea and land. The land sea breeze causes the wind to turn anticlockwise towards the road sector after the sunrise and in evening returns back to westerly. This turning may have its own effect on the pollutant concentrations measured at the SMEAR III. Air temperature had a diurnal pattern with lower values at night which increased towards the afternoon due to sun elevation (Fig. 8c).

Solar radiation is a dominant factor in annual and diurnal behaviour of most of the turbulent fluxes. From the diurnal pattern of u_* (Fig. 8d), we can see how the strength of the turbulence is higher during the daytime enabling more efficient pollutant dispersion. This pattern was pronounced in summer when the amplitude between the nocturnal and daytime u_* was 0.3 m s^{-1}. H followed the diurnal pattern of global radiation well, reaching 240 W m^{-2} during summer days (Fig. 8e). H got negative values (indicating unstable stratification of the atmosphere) during nights, except in winter when the nocturnal stratification was slightly unstable due to the anthropogenic heat sources (e.g. Salmond *et al*. 2005). Same pattern could also be distinguished

from the diurnal pattern of stability parameter (ζ in Fig. 8h). LE was low in winter and autumn, and reached 120 W m^{-2} during summer days following the development of sun elevation and growing season. The diurnal patterns of heat fluxes are also dependent on land use sectors as was shown by Vesala *et al*. (2007). The value of H was highest in the urban sector and lowest in the vegetation sector where the heat is consumed in transpiration as could be seen as elevated LE. The diurnal behaviour of H and LE followed those previously reported, even though the peak values range between 50 and 300 W m^{-2} for H and between 10 and 240 W m^{-2} for LE depending on the analyzed season (Grimmond *et al*. 2002a, Nemitz *et al*. 2002, Moriwaki and Kanda 2004).

The surrounding area acted most of the time as a source for CO_2 and F_c reached a value of 10 μmol m^{-2} s^{-1} in winter. In summer, the vegetation uptake of CO_2 exceeded the anthropogenic emissions on the footprint area (source area) resulting in downward fluxes of 3 μmol m^{-2} s^{-1}. Vesala *et al*. (2007) showed that traffic is the major source of CO_2 at our site and the highest F_c were measured in the road sector. It should be noted, that F_c is potentially slightly underestimated due to the sensor heat effect as presented by Burba *et al*. (2006). At our site, the underestimation increases with decreasing temperature reaching 2.5 μmol m^{-2} s^{-1} (Vesala *et al*. 2007). Previous studies have reported similar diurnal behaviour of F_c but downward fluxes have only been observed occasionally (Nemitz *et al*. 2002, Grimmond *et al*. 2002b, Vogt *et al*. 2006, Coutts *et al*. 2007).

From the diurnal pattern of atmospheric stability (Fig. 8h), we see how the atmospheric stratification changes from stable to unstable after the sunrise. This describes the strengthening of the turbulent mixing in the urban boundary layer after the sun starts to heat the ground. As was previously mentioned, on average, the stratification stays unstable through the day in winter. During daytime, the atmosphere was more unstable in summer than during other seasons. This enables higher mixing heights when pollutants can mix into larger air volume decreasing the concentrations above the ground.

Results from the multiple linear regression (MLR) analysis

Variables included to the final MLR models varied between the seasons. In the case of UFP, traffic rate was always included with positive effect on UFP (Table 4). The other variables present in the models were wind speed (U), mixing ratio of H_2O, temperature (T), variance of the vertical wind speed (σ_w) and south-west wind component. Even though the variables changed between the seasonal models, the same physical effects were present throughout the analyzed period. U and σ_w are indicative of mixing processes affecting the dispersion of pollutant concentrations. A weaker mixing causes higher concentrations above the ground. The H_2O concentration is proportional to T and both of them are typically lower in high pressure situations when strong inversions and high concentrations can be measured. Buzorius *et al*. (2001) reported that on new particle formation days, the H_2O mixing ratios were smaller than on non-event days having its own possible contribution to the negative correlation between H_2O and UFP in spring. The available variables explained UFP concentrations better in winter and autumn when traffic is dominating other UFP sources. During all seasons, the influence of traffic on UFP concentrations was higher on weekdays than on weekends, when the meteorological parameters became more important. In winter and spring, better MLR models were obtained for weekends than for weekdays. This might be caused by the local traffic activity at the parking lot next to the station or the construction site, which are present mainly on weekdays and which were not included on the model parameters. On weekdays, also quality of a simple model may be poorer due to the more complex distribution of sources.

For accumulation mode particles, traffic was not as dominant factor as in the case of UFP (Table 5). The effect of traffic was systematically equally or less important than the meteorological variables and in spring, traffic was not even included to the final model. The effect of traffic decreased on weekends similarly to UFP concentrations. The strong pressure dependence in spring is related to the synoptic weather situation

Table 4. Results from the multiple linear regression (MLR) analysis of ultrafine particle concentrations ($p < 0.05$). In the analysis hourly values were used and MLR models were made for each season and for weekdays and weekends, separately. Variables which were used in final models were traffic rate (Tr), wind speed (U), water vapour mixing ration (H_2O), temperature (T), wind direction component in north-south direction (WD_1) and variance of vertical wind speed (σ_w). The beta coefficients (β) and their standard deviations (σ_β), and performance indices, R^2, and root mean square error (rmse), are also listed.

		All		Weekdays		Weekends	
		β	σ_β	β	σ_β	β	σ_β
Winter	Tr	0.57	0.00	0.59	0.00	0.45	0.00
	U	–0.30	0.00	–0.31	0.00	–0.19	0.01
	H_2O	–0.42	0.00	–0.38	0.00	–0.61	0.00
	R^2 (%)	56	55	68			
	rmse	0.66 ± 0.00	0.67 ± 0.00	0.57 ± 0.00			
Spring	Tr	0.35	0.00	0.40	0.00	0.03	0.01
	U	–0.42	0.00	–0.80	0.00	–0.42	0.00
	H_2O	–0.35	0.00	–0.22	0.00	–0.67	0.01
	R^2 (%)	39	42	40			
	rmse	0.78 ± 0.00	0.76 ± 0.00	0.77 ± 0.00			
Summer	Tr	0.40	0.00	0.42	0.00	0.16	0.00
	U	–0.40	0.00	–0.44	0.00	–0.35	0.00
	T	–0.24	0.00	–0.24	0.00	–0.18	0.00
	R^2 (%)	26	30	15			
	rmse	0.86 ± 0.00	0.83 ± 0.00	0.91 ± 0.00			
Autumn	Tr	0.70	0.00	0.73	0.00	0.29	0.01
	WD_1	0.04	0.01	0.01	0.00	0.27	0.01
	σ_w	–0.21	0.00	–0.19	0.01	–0.52	0.01
	H_2O	–0.15	0.00	–0.11	0.00	–0.38	0.01
	R^2 (%)	61	64	73			
	rmse	0.62 ± 0.00	0.60 ± 0.00	0.51 ± 0.01			

Table 5. Same as in Table 4 but for accumulation mode particle concentrations ($p < 0.05$). Variables which were used in final models were traffic rate (Tr), variance of wind speed (σ_u), temperature (T), pressure (p), vertical wind speed (w), water vapour mixing ration (H_2O), variance of vertical wind speed (σ_w) and relative humidity (RH).

		All		Weekdays		Weekends	
		β	σ_β	β	σ_β	β	σ_β
Winter	Tr	0.38	0.00	0.39	0.00	0.26	0.01
	σ_u	–0.28	0.00	–0.35	0.00	–0.15	0.01
	T	–0.40	0.00	–0.34	0.00	–0.54	0.00
	R^2 (%)	33	33	35			
	rmse	0.82 ± 0.00	0.82 ± 0.00	0.80 ± 0.00			
Spring	p	0.54	0.00	0.63	0.00	0.44	0.00
	w	0.26	0.00	0.18	0.00	0.45	0.00
	R^2 (%)	40	45	43			
	rmse	0.78 ± 0.00	0.74 ± 0.00	0.74 ± 0.00			
Summer	Tr	0.22	0.00	0.24	0.00	0.15	0.00
	σ_u	–0.34	0.00	–0.31	0.00	–0.28	0.00
	H_2O	0.59	0.00	0.57	0.00	0.68	0.00
	R^2 (%)	47	41	62			
	rmse	0.73 ± 0.00	0.77 ± 0.00	0.62 ± 0.00			
Autumn	Tr	0.47	0.00	0.57	0.00	0.38	0.00
	σ_w	–0.46	0.00	–0.25	0.00	–0.33	0.00
	RH	0.36	0.00	0.58	0.00	0.07	0.00
	R^2 (%)	64	77	31			
	rmse	0.60 ± 0.00	0.48 ± 0.00	0.82 ± 0.00			

which evidently affected strongly accumulation mode particle concentrations. In summer, accumulation mode particle concentrations increased as a function of H_2O. Same was observed in the case of coarse particles (Table 6). This is most likely related to the condensation of water vapour on pre-existing particles which increase their size to larger classes. Similar results were also presented by Jamriska *et al.* (2008), who found accumulation mode particles to be strongly affected by RH with positive dependence in Brisbane, Australia. In the same study, particle concentrations with the particle size range of 15–880 nm were found to be dominated by traffic, wind speed, temperature and relative humidity similarly to our results.

Overall, the coarse particle concentrations could not be explained as well with the available variables as fine particles. The especially low R^2 in spring (9%) was most likely caused by the street dust re-suspended by wiping machines and/or traffic at the parking lot. These are not included on the available variables and are mainly present on weekdays, which would explain better models on weekends. *U* had opposite effect on coarse particles than it had on UFP. High wind speed increases the re-suspension of larger particles from ground while for smaller particles wind speed is more related to the atmospheric stability and mixing (e.g. Hussein *et al.* 2006). The appearance of west-east wind direction component in autumn was evident (*see* also Fig. 4d).

The only flux variable present in the models was LE, with an inverse effect in the case of coarse particles in spring. Re-suspension of dust is more efficient in dry conditions when also LE is expected to be lower. The momentum flux itself was not present in the models but it is directly proportional to wind speed and standard deviation of wind speed components, which were included in the final models. Stability parameter ζ was not present in any of the models (Fig. 8h). It is describing the general mixing conditions in the boundary layer and it is inadequate in point by point comparisons. Also the strong diurnal patter of ζ may have its effect. We are not aware of any study where correlations between aero-

Table 6. Same as in Table 4 but for coarse particle concentrations ($p < 0.05$). Variables which were used in final models were traffic rate (Tr), vertical wind speed (w), water vapour mixing ration (H_2O), pressure (p), latent heat flux (LE), wind speed (U) and wind direction component in east-west direction (WD_2).

		All		Weekdays		Weekends	
		β	σ_β	β	σ_β	β	σ_β
Winter	Tr	0.25	0.00	0.28	0.00	0.23	0.01
	w	0.27	0.00	0.22	0.00	0.37	0.01
	H_2O	–0.37	0.00	–0.35	0.00	–0.51	0.01
	R^2 (%)	22	25	16			
	rmse	0.88 ± 0.00	0.86 ± 0.00	0.91 ± 0.00			
Spring	Tr	0.30	0.00	0.24	0.00	0.08	0.01
	p	0.11	0.00	0.02	0.00	0.51	0.01
	LE	–0.25	0.01	–0.30	0.01	–0.13	0.01
	R^2 (%)	9	8	28			
	rmse	0.95 ± 0.00	0.96 ± 0.00	0.85 ± 0.00			
Summer	Tr	0.18	0.00	0.22	0.00	–0.12	0.00
	w	0.05	0.00	0.03	0.00	0.22	0.00
	H_2O	0.41	0.00	0.33	0.00	0.49	0.00
	R^2 (%)	21	16	37			
	rmse	0.88 ± 0.00	0.92 ± 0.00	0.79 ± 0.00			
Autumn	Tr	0.46	0.00	0.48	0.01	0.15	0.01
	U	0.21	0.01	0.36	0.01	–0.11	0.01
	WD_2	0.12	0.01	0.14	0.01	0.18	0.01
	T	0.27	0.01	0.12	0.01	0.70	0.01
	R^2 (%)	39	44	46			
	rmse	0.78 ± 0.00	0.75 ± 0.00	0.73 ± 0.00			

sol particle number concentrations and turbulent fluxes have been studied in urban areas. Thus, we do not know are the observed correlations typical for urban areas or only characteristic to our measurement site.

Correlations between aerosol particle number concentrations and NO_x, CO and SO_2

Linear correlations of UFP and accumulation mode particle concentrations with NO_x, CO and SO_2 concentrations were studied separately for each season between December 2006 and June 2007 (Table 7). All concentrations were logarithmically transformed before the analysis.

Both UFP and accumulation mode particle concentrations correlated better with NO_x and CO than with SO_2 pointing out the importance of traffic as a source of fine particles. Similar results have also been reported by Morawska *et al*. (1998) and Roth *et al*. (2008). The correlation of UFP with NO_x and CO increased in winter indicating the increased effect of traffic due to e.g. lowered mixing. NO_x correlated better with UFP than with accumulation mode particles, while CO correlated better with accumulation mode particles. Both NO_x and UFP represent primary emissions from combustion sources whose concentrations are high near emissions sources (NO_x chemistry fast). The lifetime of CO in the atmosphere is of the same order of magnitude as the lifetime of accumulation mode particles (Seinfeld and Pandis 1998), which explains the higher correlation between these two. Contrary to our results, Roth *et al*. (2008) found higher NO_x correlation with accumulation mode particles (size range of 0.1–0.62 μm) than with UFP in Strasbourg, France. The difference might rise due to the logarithmic transformation used in this study. Previously, UFP have been found to correlate better with CO than with NO_x (Morawska *et al*. 1998, Noble *et al*. 2003). In Helsinki, the local emissions of CO are lower as compared with the emissions in these larger cities and, thus, the effect of transported CO likely more evident.

SO_2 correlated better with fine particles in spring and summer than in winter and autumn. SO_2 is considered to be a precursor gas for new particle formation in the atmosphere, as it oxides to sulphuric acid which is tied to nucleation of new particles (Kulmala 2003, Kulmala *et al*. 2004, Kulmala *et al*. 2006). Jeong *et al*. (2004) found a good correlation between UFP and SO_2 during nucleation events. This could at least partly explain the higher correlation of UFP and SO_2 in spring and summer. However, longer time series of SO_2 and CO are needed for more detailed analysis of the connection between these gases and aerosol particle number concentrations.

Conclusions

Here we report results from the air pollution and turbulent exchange measurements made at the urban measurement station SMEAR III. UFP, accumulation mode particle and coarse particle number concentrations, concentrations of gaseous pollutants (O_3, NO_x, CO and SO_2), turbulent fluxes of momentum, heat, H_2O and CO_2 and meteorological were analyzed on annual and diurnal basis. The measurements of fine aerosol particles (UFP and accumulation mode particles) and meteorological variables were started in August 2004 while the other measurements have been gradually added with time. In this study, the data until June 2007 were analyzed. The wind direction dependencies of pollutant concentrations were analyzed and the effect of traffic, turbulent fluxes and meteorological variables on

Table 7. Squared correlation coefficients (R^2) from a linear fitting (p = 0.00) made between aerosol particle number concentration of ultrafine particles (UFP) and accumulation mode particles (AP), and the gas pollutants of NO_x, CO and SO_2. Data in December 2005–June 2007 was used in the analysis.

		NO_x	CO	SO_2
Winter	UFP	0.74	0.36	0.17
	AP	0.55	0.69	0.22
Spring	UFP	0.45	0.15	0.28
	AP	0.63	0.42	0.36
Summer	UFP	0.54	0.23	0.28
	AP	0.28	0.35	0.25
Autumn	UFP	0.69	0.24	0.01
	AP	0.48	0.63	0.08

aerosol particle number concentrations was studied by means of a multiple regression analysis. Besides, correlations between fine particles and gas concentrations of NO_x, CO and SO_2 were analyzed.

The pollutant concentrations of UFP, accumulation mode particles, NO_x, CO and SO_2 showed a distinct annual pattern with highest concentrations in winter due to poor pollutant mixing and increased emissions from stationary combustions sources. The annual behaviour of accumulation mode particles is also related to the effect of long-range transport which was pronounced during the summer season. The coarse particle concentration peaked after the melting of snow and ice in spring when the re-suspension by traffic and wiping-machine induced turbulence is most efficient. At the measurement site, the land use cover had a clear effect on the measured traffic related pollutants (UFP, accumulation mode particles, NO_x and CO) with highest values in the road sector and lowest in the vegetation sector. The diurnal patterns were consistent with vehicular activity and the highest weekday concentrations were measured during the morning rush hour. Considering these pollutant concentrations, Helsinki seem to be a relatively clean city when compared with other cities around the world. However, so far there has been limited amount of studies which simultaneously measure both size-fractioned aerosol particle number concentrations and gas pollutants. Thus, more measurements are needed for more detailed comparisons.

The annual patterns of O_3, H and LE followed strongly the amount of available solar radiation as they increased towards summer. O_3 concentrations were also affected by the amount of the O_3-consuming compound which could be seen as lower weekday concentrations. The friction velocity (u_*) and F_c did not have a distinct annual pattern and on average the urban cover acted as a source for CO_2 around the year. However, from the diurnal behaviour of F_c could be seen that in the footprint area during the growing season the vegetation uptake of CO_2 exceeded the emissions from anthropogenic sources which could be seen as downward fluxes. The stratification of nocturnal boundary layer was unstable during the winter due to the anthropogenic heat sources. During other seasons, the nocturnal stratification remained stable. The atmosphere was most unstable during the summer days indicating stronger turbulent mixing. The enhanced mixing during summer months as compared with that during winter months tends to decrease pollutant concentrations as observed. On the other hand, also emissions during summer months are lower.

Variations in UFP were most affected by traffic as was shown by the MLR analysis. However, this effect decreased on weekends when the meteorological parameters, especially turbulent mixing, became more important. Poorer MLR models were obtained for weekday than for weekend concentrations in winter and autumn most probably due to the emissions just next to the measurement station, which are not included in traffic counts and are present only on weekdays. On weekdays also the quality of a simple model may be reduced. The importance of traffic as a source of aerosol particles decreased with increasing particle size when the prevailing meteorological conditions and H_2O mixing ratios became more important. Turbulent mixing had always effect on the aerosol particle number concentrations and its effect depended on the size of the particle. High wind speed increases the mechanical mixing and air pollutants can mix into larger air volume decreasing the pollutant concentrations above ground. On the other hand, higher mixing re-suspends large particles into air and thus increases their concentrations.

Correlations between fine particles and CO and NO_x were better than with SO_2 addressing the importance of traffic as a source of these particles. The effect of long-range transport on accumulation mode particles and CO was seen as increased correlation between these two. UFP and NO_x on the other hand are primary emitted and get their highest concentrations near pollution sources which increased their correlation. The correlation between SO_2 and both aerosol particle size classes improved in spring and summer and in the case of UFP, higher correlation is likely related to new particle formation events.

Acknowledgements: For financial support we thank Maj and Tor Nessling Foundation, National technology Agency (TEKES, Ubicasting project), URPO and REBECCA by Helsinki University Environmental Research Centre (HERC),

Nordic Centre of Excellence's BACCI and NECC, the Academy of Finland Center of Excellence program (project no. 1118615), CarboEurope and IMECC.

References

Aalto P., Hämeri K., Becker E., Weber R., Salm J., Mäkelä J., Hoell C., O'Dowd C., Karlsson H., Hansson H.-C., Väkevä M., Koponen I.K., Buzorius G. & Kulmala M. 2001. Physical characterization of aerosol particles during nucleation events. *Tellus B* 53B: 344–358.

Aalto P., Hämeri K., Paatero P., Kulmala M., Bellander T., Berglind N., Bouso L., Castaño-Vinyals G., Sunyer J., Cattani G., Marconi A., Cyrys J., von Klot S., Peters A., Zetzsche K., Lanki T., Pekkanen J., Nyberg F., Sjövall B. & Forastiere F. 2005. Aerosol particle concentration measurements in five European cities using TSI-3022 Condensation Particle Counter over a three-year period during health effects of air pollution on susceptible subpopulations. *J. Air Waste Manage. Assoc.* 55: 1064–1076.

Amoroso A., Beine H.J., Esposito G., Perrino C., Catrambone M. & Allegrini I. 2008. Seasonal differences in atmospheric nitrous acid near Mediterranean urban areas. *Water Air Soil Pollut.* 188: 81–92.

Aubinet M., Grelle A., Ibrom A., Rannik Ü., Moncrieff J., Foken T., Kowalski A.S., Martin P.H., Berbigier Ch., Bernhofer Ch., Clement R., Elbers J., Granier A., Grünwald T., Morgenstern K., Pilegaard K., Rebmann C., Snijders W., Valentini R. & Vesala T. 2000. Estimates of the annual net carbon and water exchange of European forests: the EUROFLUX methodology. *Adv. Ecol. Res.* 30: 114–175.

Burba G. Anderson D., Liukang X. & McDermitt D. 2006. Correcting apparent off-season CO_2 uptake due to surface heating of an open path gas analyzer: progress report of an ongoing study. In: *Proceedings of the 27th Annual Conference of Agricultural and Forest Meteorology*, Amer. Met. Soc., San Diego, California, USA, pp. 1–13.

Buzorius G., Rannik Ü., Nilsson D. & Kulmala M. 2001. Vertical fluxes and micrometeorology during aerosol particle formation events. *Tellus* 53B: 394–405.

Coceal O. & Belcher S.E. 2004. A canopy model of mean winds through urban areas. *Quart. J. Roy. Meteorol. Soc.* 130: 1349–1372.

Coutts A.M., Beringer J. & Tapper N. 2007. Characteristics influencing the variability of urban CO_2 fluxes in Melbourne, Australia. *Atmos. Environ.* 41: 51–62.

Cros B., Durand P., Cachier H., Drobinski Ph., Fréjafon E., Kottmeier C., Perros P.E., Peuch V.-H., Ponche J.-L., Robin, D., Saïd F., Toupance G. & Wortham H. 2004. The ESCOMPTE program: an overview. *Atmos. Res.* 69: 241–279.

Curtis L., Rea W., Smith-Willis P., Fenyves E. & Pan Y. 2006. Adverse health effects of outdoor air pollutants. *Environment International* 32: 815–830.

Dal Maso M., Kulmala M., Riipinen I., Wagner R., Hussein T., Aalto P.P. & Lehtinen K. 2005. Formation and growth of fresh atmospheric aerosols: eight years of aerosol size distribution data from SMEAR II, Hyytiälä, Finland. *Boreal. Env. Res.* 10: 323–336.

Drebs A., Nordlund A., Karlsson P., Helminen J. & Rissanen P. 2002. *Tilastoja Suomen ilmastosta 1971–2000*. Ilmatieteen laitos, Helsinki.

Foken T.H. & Wichura B. 1996. Tools for quality assessment of surface-based flux measurements. *Agric. For. Meteorol.* 78: 83–105.

Grimmond C.S.B. & Oke T. 2002. Turbulent heat fluxes in urban areas: Observations and a local scale urban meteorological parameterization scheme (LUMPS). *J. Appl. Meteorol.* 41: 792–807.

Grimmond C.S.B., King T.S., Cropley F.D., Nowak D.J. & Souch C. 2002. Local-scale fluxes of carbon dioxide in urban environments: methodological challenges and results from Chicago. *Environmental Pollution* 116: 243–254.

Grimmond C.S.B., Salmond J.A., Oke T.R., Offerle B. & Lemonsu A. 2004. Flux and turbulence measurements at a dense urban site in Marseille: Heat, mass (water, carbon dioxide) and momentum. *J. Geophys. Res.* 109, D24, D24101, doi: 10.1029/2004JD004936.

Hair J.F., Black W.C, Babin B.J., Anderson R.E. & Tatham R.L. 2006. *Multivariate data analysis*, 6th ed. Pearson Education Inc., New Jersey.

Hanna S. & Britter R. 2002. *Wind flow and vapor cloud dispersion at industrial and urban sites*. Center for Chemical Process Safety/AIChE.

Hari P. & Kulmala M. 2005. Station for Measuring Ecosystem–Atmosphere Relations (SMEAR II). *Boreal. Env. Res.* 10: 315–322.

Hari P., Kulmala M., Pohja T., Lahti T., Siivola E., Palva L., Aalto P., Hämeri K., Vesala T., Luoma S. & Pulliainen E. 1994. Air pollution in eastern Lapland: challenge for an environmental measurement station. *Silva Fennica* 28: 29–39.

Harrison R.M. & Jones A.M. 2005. Multisite study of particle number concentrations in urban air. *Environ. Sci. Technol.* 39: 6063–6070.

Hussein T., Johansson C., Karlsson H. & Hansson H.-C. 2008. Factors affecting non-tailpipe aerosol emissions from paved roads: on-road measurements in Stockholm, Sweden. *Atmos. Environ.* 42: 688–702.

Hussein T., Karppinen A., Kukkonen J., Härkönen J., Aalto P., Hämeri K., Kerminen V.-M. & Kulmala M. 2006. Meteorological dependence of size-fractionated number concentrations of urban aerosol particles. *Atmos. Environ.* 40: 1427–1440.

Jamriska M., Morawska L. & Mergersen K. 2008. The effect of temperature and humidity on size segregated traffic exhaust particle emissions. *Atmos. Environ.* 42: 2369–2382.

Jeong C.-H., Hopke P.K., Chalupa D. & Utell M. 2004. Characteristics of nucleation and growth events of ultrafine particles measured in Rochester, NY. *Environ. Sci. Technol.* 38: 1933–1940.

Ketzel M., Wåhlin P., Kristensson A., Swietlicli E., Berkowicz R., Nielsen O.J. & Palmgren F. 2004. Particle size distribution and particle mass measurements at urban, near-city and rural level in the Copenhagen area and

southern Sweden. *Atmos. Chem. Phys.* 4: 281–292.

Khlystov A., Stanier C. & Pandis S.N. 2004. An algorithm for combining electrical mobility and aerodynamic size distributions data when measuring ambient aerosol. *Aerosol Sci. Technol.* 38: 229–238.

Klumpp A., Ansel W., Klumpp G., Calatayud V., Garrec J.P., He S., Peñuelas J., Ribas À., Ro-Poulsen H., Rasmussen S., Sanz M. & Vergne P. 2006. Ozone pollution and ozone biomonitoring in European cities. Part I: Ozone concentrations and cumulative exposure indices at urban and suburban sites. *Atmos. Environ.* 40: 7963–7974.

Kulmala M. 2003. How particles nucleate and grow. *Science* 302: 1000–1001.

Kulmala M., Lehtinen K.E.J. & Laaksonen A. 2006. Cluster activation theory as an explanation of the linear dependence between formation rate of 3 nm particles and sulphuric acid concentration. *Atmos. Chem. Phys.* 6: 787–793.

Kulmala M., Vehkamäki H., Petäjä T., Dal Maso M., Lauri A., Kerminen V.-M., Birmili W. & McMurry P. 2004. Formation and growth rates of ultrafine atmospheric aerosols: a review of observations. *J. Aerosol Sci.* 35: 143–176.

Kupiainen K., Tervahattu H. & Räisänen M. 2003. Experimental studies about the impact of traction sand on urban road dust composition. *Sci. Total Environ.* 308: 175–184.

Laakso L., Hussein T., Aarnio P., Komppula M., Hiltunen V., Viisanen Y. & Kulmala M. 2003. Diurnal and annual characteristics of particle mass and number concentrations in urban, rural and arctic environments in Finland. *Atmos. Environ.* 37: 2629–2641.

McMurry P.H., Wang X., Park K. & Ehara K. 2002. The relationship between mass and mobility for atmospheric particles: A new technique for measuring particle density. *Aerosol Sci. Technol.* 36: 227–238.

Morawska L., Thomas S., Bofinger N., Wainwright D. & Neale D. 1998. Comprehensive characterization of aerosols in a subtropical urban atmosphere: particle size distribution and correlation with gaseous pollutants. *Atmos. Environ.* 32: 2467–2478.

Moriwaki R. & Kanda M. 2004. Seasonal and diurnal fluxes of radiation, heat, water vapour, and carbon dioxide over a suburban area. *J. Appl. Meteorol.* 43: 1700–1710.

Myllynen M., Haaparanta S., Julkunen A., Koskentalo T., Kousa A. & Aarnio P. 2007. *Ilmanlaatu pääkaupunkiseudulla vuonna 2006*. YTV Pääkaupunkiseudun Yhteistyövaltuuskunta, YTV:n julkaisuja 12/2007.

Nel A. 2005. Air pollution-related illness: effects of particles. *Science* 308: 804–806.

Nemitz E., Hargreaves K.J., McDonald A.G., Dorsey J. & Fowler D. 2002. Micrometeorological measurements of the urban heat budget and CO_2 emissions on a city scale. *Environ. Sci. Technol.* 36: 3139–3146.

Noble C.A., Mukerjee S., Gonzales M., Rodes C, Lawless P, Natarajan S., Myers E, Norris G., Smith L., Özkaynak H. & Neas L. 2003. Continuous measurement of fine and ultrafine particulate matter, criteria pollutants and meteorological conditions in urban El Paso, Texas. *Atmos. Environ.* 37: 827–840.

Norman M. & Johansson C. 2006. Studies of some measures to reduce road dust emissions from paved roads in Scandinavia. *Atmos. Environ.* 40: 6154–6164.

Oke T.R. 1982. The energetic basis of the urban heat island. *Quart. J. Roy. Meteorol. Soc.* 108: 1–24.

Oke T.R., Cleugh H.A., Grimmond S., Schmid H.P. & Roth M. 1989. Evaluation of spatially averaged fluxes of heat, mass and momentum in the urban boundary layer. *Weather and Climate* 9: 14–21.

Pakkanen T., Loukkola K., Korhonen C., Aurela M., Mäkelä T., Hillamo R., Aarnio P., Koskentalo T., Kousa A. & Maenhaut W. 2001. Sources and chemical composition of atmospheric fine and coarse particles in the Helsinki area. *Atmos. Environ.* 35: 5381–5391.

Rantamäki M., Sofiev N., Eresmaa N., Saarikoski S., Mäkelä T., Hillamo R., Sarkanen A., Kukkonen J. & Karppinen A. 2007. Evaluation of severe air quality episode in Helsinki in August 2006, caused by regionally transported smoke. In: *Abstracts of the 6th International Conference on Urban Air Quality, 27–29 March, Cyprus*, University of Hertfordshire, UK, p. 91.

Roth M. 2000. Review of atmospheric turbulence over cities. *Quart. J. R. Met. Soc.* 126: 941–990.

Roth E., Kehrli D., Bonnot K. & Trouvé G. 2008. Size distributions of fine and ultrafine particles in the city of Strasbourg: Correlation between number of particles and concentrations of NO_x and SO_2 gases and some soluble ions concentration determination. *Journal of Environmental Management* 86: 282–290.

Ruuskanen J., Tuch Th., Ten Brink H., Peters A., Khlystov A., Mirme A., Kos G.P.A., Brunekreef B., Wichmann H.E., Buzorius G., Vallius M., Kreyling W.G. & Pekkanen J. 2001. Concentrations of ultrafine, fine and $PM_{2.5}$ particles in three European cities. *Atmos. Environ.* 35: 3729–3738.

Salmond J.A., Oke, T.R., Grimmond C.S.B., Roberts S. & Offerle B. 2005. Venting of heat and carbon dioxide from urban canyons at night. *J. Appl. Meteorol.* 44: 1180–1194.

Seinfeld J.H. & Pandis S.N. 1998. *Atmospheric chemistry and physics*. John Wiley & Sons, New York.

Shi Z.B., He K.E., Yu X.C., Yao Z.L., Yang F.M., Ma Y.L., Ma R., Jia Y.T. & Zhang J. 2007. Diurnal variation of number concentration and size distribution of ultrafine particles in the urban atmosphere of Beijing in winter. *J. Env. Sci.* 19: 933–938.

Sillanpää M., Saarikoski S., Hillamo R., Pennanen A., Makkonen U., Spolnik Z., Van Grieken R., Koskentalo T.A. & Salonen R.O. 2005. Chemical composition, mass size distribution and source analysis of long-range transported wild fire smokes in Helsinki. *Sci. Total Environ.* 350: 119–135.

Sillman S. 1999. The relation between ozone, NO_x and hydrocarbons in urban and polluted rural environments. *Atmos. Environ.* 33: 1821–1845.

Soegaard H. & Møller-Jensen L. 2003. Towards a spatial CO_2 budget of a metropolitan region based on textural image classification and flux measurements. *Remote Sensing of Environment* 87: 283–294.

Stein S.W., Turpin B.J., Cai X.P., Huang C. & McMurry

P.H. 1994. Measurements of relative humidity-dependent bounce and density for atmospheric particles using the DMA-impactor technique. *Atmos. Environ.* 28: 1739–1746.

Suni T., Rinne J., Reissel A., Altimir N., Keronen P., Rannik Ü., Dal Maso M., Kulmala M. & Vesala T. 2003. Long-term measurements of surface fluxes above a Scotch pine forest in Hyytiälä southern Finland, 1996–2001. *Boreal Env. Res.* 8: 287–301.

Vesala T., Järvi L., Launiainen S., Sogachev A., Rannik Ü., Mammarella I., Siivola E., Keronen P., Rinne J., Riikonen A. & Nikinmaa E. 2007. Surface–atmosphere interactions over complex urban terrain in Helsinki, Finland. *Tellus* 60B: 188–199.

Vogt R., Christen A., Rotach M., Roth M. & Satyanarayana A. 2006. Temporal dynamics of CO_2 fluxes and profiles over a central European city. *Theor. Appl. Climatol.* 84: 117–126.

Young L.-H. & Keeler G. 2007. Summertime ultrafine particles in urban and industrial air: aitken and nucleation mode particle events. *Aerosol and Air quality Research* 7: 379–402.

Webb E.K., Pearman G.I. & Leuning R. 1980. Correction of flux measurements for density effects due to heat and water vapour transfer. *Quart. J. Roy. Meteorol. Soc.* 106: 85–100.

Wehner B. & Wiedensohler A. 2003. Long term measurements of submicrometer urban aerosols: statistical analysis for correlations with meteorological conditions and trace gases. *Atmos. Chem. Phys.* 3: 867–879.

Woo K.S., Chen D.R., Pui D.Y.H. & McMurry P.H. 2001. Measurement of Atlanta aerosol size distributions: Observations of ultrafine particle events. *Aerosol Sci. Technol.* 34: 75–87.